

Two 'b's in the Beehive: The Discovery of the First Hot Jupiters in an Open Cluster

SAMUEL N. QUINN¹, RUSSEL J. WHITE¹, DAVID W. LATHAM², LARS A. BUCHHAVE^{3,4}, JUSTIN R. CANTRELL¹, SCOTT E. DAHM⁵, GABOR FÚRÉSZ², ANDREW H. SZENTGYORGYI², JOHN C. GEARY², GUILLERMO TORRES², ALLYSON BIERYLA², PERRY BERLIND², MICHAEL C. CALKINS², GILBERT A. ESQUERDO², ROBERT P. STEFANIK²

Draft version July 9, 2018

ABSTRACT

We report the discovery of two giant planets orbiting stars in Praesepe (also known as the Beehive Cluster). These are the first known hot Jupiters in an open cluster and the only planets known to orbit Sun-like, main-sequence stars in a cluster. The planets are detected from Doppler shifted radial velocities; line bisector spans and activity indices show no correlation with orbital phase, confirming the variations are caused by planetary companions. Pr0201b orbits a $V = 10.52$ late F dwarf with a period of 4.4264 ± 0.0070 days and has a minimum mass of $0.540 \pm 0.039 M_{\text{Jup}}$, and Pr0211b orbits a $V = 12.06$ late G dwarf with a period of 2.1451 ± 0.0012 days and has a minimum mass of $1.844 \pm 0.064 M_{\text{Jup}}$. The detection of 2 planets among 53 single members surveyed establishes a lower limit on the hot Jupiter frequency of $3.8_{-2.4}^{+5.0}\%$ in this metal-rich open cluster. Given the precisely known age of the cluster, this discovery also demonstrates that, in at least 2 cases, giant planet migration occurred within 600 Myr after formation. As we endeavor to learn more about the frequency and formation history of planets, environments with well-determined properties – such as open clusters like Praesepe – may provide essential clues to this end.

Subject headings: open clusters and associations: individual (Praesepe, M44, NGC 2632, Beehive) — planetary systems — stars: individual (BD+20 2184, 2MASS J08421149+1916373)

1. INTRODUCTION

Exoplanet studies over the last 15 years have demonstrated that at least 10% of FGK stars harbor gas giant planets, with many of them at surprisingly small separations, implying inward migration after formation (Wright et al. 2011). Although the mechanism by which most planets migrate is not understood, powerful constraints on proposed theories of migration can be established by determining the orbital properties of planets at young or adolescent ages (< 1 Gyr). For example, if migration occurs primarily due to interactions with a circumstellar disk (e.g., Goldreich & Tremaine 1980; Lin et al. 1996), the migration must occur before the disk dissipates (~ 10 Myr; Carpenter et al. 2006), and is predicted to circularize orbits. Alternatively, if migration occurs primarily due to planet-planet scattering (e.g., Adams & Laughlin 2003), the process may take hundreds of millions of years to occur and can produce highly eccentric orbits, prior to any tidal circularization (see review by Lubow & Ida 2010).

A direct way to find planets that can potentially be used to constrain theories of migration is to search for them in young open clusters. However, until now, only 2 open cluster stars were known to harbor planets – ϵ Tau in the Hyades (Sato et al. 2007) and TYC 5409-2156-1

in NGC 2423 (Lovis & Mayor 2007) – both of which are giant stars and thus, by necessity, have planets on wider orbits than those occupied by hot Jupiters. In both cases the host stars are of intermediate mass (2.7 and $2.4 M_{\odot}$), likely A or B type stars when on the main sequence. The lack of detected planets orbiting FGK main sequence stars (which are often referred to as Sun-like stars) in open clusters has remained despite radial velocity (RV) surveys of 94 dwarfs in the metal-rich Hyades (Paulson et al. 2004, mean $[\text{Fe}/\text{H}] = +0.13$) and 58 dwarfs in M67 (Pasquini et al. 2012), as well as numerous transit searches in other clusters (e.g., Hartman et al. 2009; Pepper et al. 2008; Mochejska et al. 2006). While the lack of detections may still be the result of small sample sizes (e.g., van Saders & Gaudi 2011), millimeter-wave studies of disks around stars in the Orion star forming region, which may evolve into an open cluster, offer a plausible astrophysical explanation. Eisner et al. (2008) find that most solar-type stars in this region do not possess disks massive enough to form gas giant planets. One may also speculate that for the few stars capable of forming planets, the remaining disk masses may be insufficient to permit inward migration (see also Debes & Jackson 2010).

In an attempt to (1) more confidently determine whether planet formation and/or migration is inhibited around stars within clusters, and (2) potentially discover planets with known ages and measurable orbital properties, we have carried out an RV survey of stars in the Praesepe open cluster. Here we present the seminal result of that survey - the discovery of the first 2 hot Jupiters orbiting Sun-like stars in a cluster.

2. SAMPLE SELECTION

Stars were selected from the Praesepe open cluster because it is relatively nearby (170 pc), has ~ 1000

¹ Department of Physics & Astronomy, Georgia State University, PO Box 4106, Atlanta, GA 30302

² Harvard-Smithsonian Center for Astrophysics, 60 Garden St, Cambridge, MA 02138

³ Niels Bohr Institute, University of Copenhagen, DK-2100 Copenhagen, Denmark

⁴ Centre for Star and Planet Formation, Natural History Museum of Denmark, University of Copenhagen, DK-1350 Copenhagen, Denmark

⁵ W. M. Keck Observatory, 65-1120 Mamalahoa Hwy, Kamuela, HI 96743

TABLE 1
TARGET LIST AND OBSERVATIONS SUMMARY

Star	α (J2000)	δ (J2000)	V (mag)	N	σ_{obs} (m s^{-1})
Pr0044	08 : 34 : 59.6	+21 : 05 : 49.2	11.06	6	42.0
Pr0047	08 : 35 : 17.8	+19 : 38 : 10.2	12.24	5	13.4
Pr0051	08 : 35 : 54.5	+18 : 08 : 57.8	10.88	5	18.3

NOTE. — Table 1 is presented in its entirety in the online journal. A portion is presented here for guidance regarding its form and content.

known members, a well determined age (600 Myr; Hambly et al. 1995; Kraus & Hillenbrand 2007; An et al. 2007; Gáspár et al. 2009; Delorme et al. 2011), and significantly elevated metallicity ($[\text{Fe}/\text{H}] = +0.27 \pm 0.10$ dex, Pace et al. 2008; $[\text{Fe}/\text{H}] = +0.11 \pm 0.03$, An et al. 2007). Its high metallicity is important because giant planet frequency is strongly correlated with host star metallicity (Santos et al. 2004; Fischer & Valenti 2005; Johnson et al. 2010); a metallicity as high as +0.27 dex implies an increase in the giant planet frequency of a factor of nearly 4 relative to solar metallicity. If this correlation applies to open cluster stars, as many as 1 in 20 Praesepe stars could harbor a hot Jupiter, and 1 in 400 could host a transiting giant planet.

Cluster members were selected from the membership list assembled by Kraus & Hillenbrand (2007), excluding stars with known spectroscopic or visual companions (Mermilliod et al. 2009; Bouvier et al. 2001; Patience et al. 2002). To ensure the velocity precision would be sufficient to detect substellar companions, we limited our initial search to slowly rotating, bright stars ($v \sin i < 12 \text{ km s}^{-1}$; $V < 12.3$). After applying these cuts, our sample contained 65 stars. Initial RV measurements revealed 12 stars to be obvious spectroscopic binaries ($\Delta\text{RV} \gg 1 \text{ km s}^{-1}$) or non-members ($|\text{RV} - \text{RV}_{\text{cluster}}| > 5 \text{ km s}^{-1}$), leaving 53 viable targets for our search. These 53 stars are listed in Table 1.

3. OBSERVATIONS

We used the Tillinghast Reflector Echelle Spectrograph (TRES; Fűrész 2008) mounted on the 1.5-m Tillinghast Reflector at the Fred L. Whipple Observatory on Mt. Hopkins, AZ to obtain high resolution spectra of Praesepe stars, between UT 6-Jan-2012 and 16-Apr-2012. TRES is a temperature-controlled, fiber-fed instrument with a resolving power of $R \sim 44,000$ and a wavelength coverage of $\sim 3850\text{-}9100 \text{ \AA}$, spanning 51 echelle orders.

We aimed to observe each target on two to three consecutive nights, followed by another two to three consecutive nights ~ 1 week later. This strategy should be sensitive to most massive planets with periods up to 10 days. Though we were sometimes forced to deviate from the planned observing cadence because of weather and instrument availability, we were able to obtain 5–6 spectra of each of our 53 targets. Exposure times ranged from 3–30 minutes, yielding a typical SNR per resolution element of ~ 40 . We also obtained nightly observations of the IAU RV standard star HD 65583, which is ~ 14 degrees from Praesepe. Precise wavelength calibration was established by obtaining ThAr emission-line spectra before and after each spectrum, through the same fiber as the science exposures.

4. ANALYSIS

4.1. Spectroscopic Reduction and Cross Correlation

Spectra were optimally extracted, rectified to intensity vs. wavelength, and for each star the individual spectra were cross-correlated, order by order, using the strongest exposure of that star as a template (for details, see Buchhave et al. 2010). We typically used ~ 25 orders, rejecting those plagued by telluric absorption, fringing far to the red, and low SNR far to the blue. For each epoch, the cross correlation functions (CCFs) from all orders were added and fit with a Gaussian to determine the relative RV for that epoch. Internal error estimates (which include, but may not be limited to, photon noise) for each observation were calculated as $\sigma_{int} = \text{RMS}(\vec{v})/\sqrt{N}$, where \vec{v} is the RV of each order, N is the number of orders, and RMS denotes the root-mean-squared velocity difference from the mean.

To evaluate the significance of any potential velocity variation, we compared the observed velocity dispersions (σ_{obs}), illustrated in Figure 1, to the combined measurement uncertainties, which we assumed stem from three sources: (1) internal error, σ_{int} (described above), (2) night-to-night instrumental error, σ_{TRES} , and (3) RV jitter induced by stellar activity, σ_* .

Before assessing the instrumental error, we first used observations of HD 65583 to correct for any systematic velocity shifts between runs (such as a 25 m s^{-1} offset caused by a shutter upgrade in mid-March). This was done by determining the median RV of HD 65583 for each run, and adjusting all RVs from that run by the amount required to make the median RV of HD 65583 constant over all runs. After applying this correction, the RMS of the HD 65583 RVs was 10.8 m s^{-1} , with internal errors of only 6 m s^{-1} . Since we expect negligible stellar jitter for the RV standard, we estimate the instrumental floor error to be $\sigma_{TRES} = \sqrt{10.8^2 - 6^2} \text{ m s}^{-1} = 9 \text{ m s}^{-1}$.

In many cases the observed velocity dispersions are too large to be explained by internal and instrumental errors alone, implying substantial stellar jitter. We calculate the stellar jitter, $\sigma_* = \sqrt{\sigma_{obs}^2 - \sigma_{int}^2 - \sigma_{TRES}^2}$. The mean stellar jitter is 13 m s^{-1} , which is similar to that found by Paulson et al. (16 m s^{-1}) for coeval Hyades members.

Accounting for internal, instrumental, and stellar noise, we constructed a χ^2 fit of each star’s RVs assuming a constant velocity, and then calculated $P(\chi^2)$, the probability that the observed χ^2 value would arise from a star of constant RV. Pr0201 (BD+20 2184) and Pr0211 (2MASS J08421149+1916373) stood out, with $P(\chi^2) < 0.001$. We obtained additional spectra of these stars, and in both cases a Lomb-Scargle periodogram revealed significant periodicity. Their radial velocities are presented in Table 2.

4.2. Orbital Solutions

We used a Markov Chain Monte Carlo (MCMC) analysis to fit Keplerian orbits to the radial velocity data of Pr0201 and Pr0211, fitting for orbital period P , time of conjunction T_c , the radial velocity semi-amplitude K , the center-of-mass velocity γ , and the orthogonal quantities $\sqrt{e} \cos \omega$ and $\sqrt{e} \sin \omega$, where e is eccentricity and ω is the argument of periastron. We calculated errors from the extent of the central 68.3% interval of the MCMC

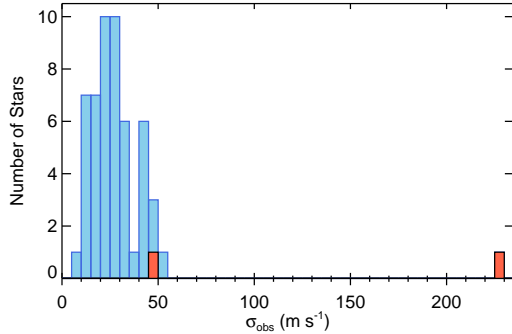


FIG. 1.— Observed velocity dispersions of the 53 stars in our sample. The two planet hosts are indicated by the solid red boxes. We note that while Pr0201 resides in the upper tail of the distribution, other stars with similar RMS values do not necessarily host two planets; large internal errors and larger than average jitter are two possible reasons for a large RMS. For reference, a $1 M_{\text{JUP}}$ planet in a 3 day orbit around a $1 M_{\odot}$ star has a full orbital amplitude of 281.7 m s^{-1} .

TABLE 2
RELATIVE RADIAL VELOCITIES OF PLANET HOSTS

BJD (−2455900)	RV (m s^{-1})	σ_{RV}	BJD (−2455900)	RV (m s^{-1})	σ_{RV}
Pr0201					
32.841253	−34.7	18.6	94.824805	19.0	20.2
33.821938	67.3	23.9	96.733645	139.4	18.7
34.857994	48.0	21.8	97.744411	−66.6	17.7
39.945964	−42.6	20.2	98.649923	−63.6	29.6
41.020182	−49.5	27.0	121.701500	−7.3	22.9
57.905296	−8.2	21.4	122.646374	81.9	17.3
58.785164	−29.3	20.1	123.637192	49.5	16.1
59.818953	0.0	12.0	124.646740	−6.3	14.0
60.759119	30.1	17.0	125.693014	−4.1	16.4
70.971372	−18.7	24.6	126.718364	47.8	30.4
71.796286	−51.7	42.5	128.683648	7.1	18.3
72.970059	13.5	29.8	129.690867	13.7	18.4
81.771272	8.6	23.5	130.724779	89.9	23.6
82.697156	87.5	15.9	131.705049	85.2	20.7
84.894042	−90.5	18.9	132.735355	48.4	24.8
86.805010	27.0	19.6	133.638578	−18.2	12.0
87.644768	102.1	19.6			
Pr0211					
86.772462	−75.7	19.1	124.663763	212.0	21.4
87.720167	413.8	13.8	125.714331	113.1	16.9
88.721641	−193.0	21.3	126.737245	275.7	30.0
96.712491	311.8	24.9	128.698449	428.7	18.2
97.756832	0.0	13.8	129.716113	−52.5	21.0
98.662801	405.8	14.7	130.741942	480.6	26.5
121.718407	346.4	18.9	131.720488	−156.9	50.5
122.663113	108.0	20.3	132.715068	504.4	24.7
123.652317	208.1	21.8	133.654723	−98.1	19.9

NOTE. — The errors listed here are internal error estimates, but in the orbital solutions we include an assumed stellar jitter of 13 m s^{-1} and an instrumental floor error of 9 m s^{-1} , added in quadrature with the internal errors.

posterior distributions.

The full orbital solutions give eccentricities of $e = 0.156^{+0.041}_{-0.112}$ for Pr0201 and $e = 0.046^{+0.021}_{-0.024}$ for Pr0211. However, it can take many precise observations to accurately measure small, non-zero eccentricities (e.g., Zakamska et al. 2011), and both are consistent with $e = 0$ to within $2\text{-}\sigma$, so we advise caution to not over-interpret these results; for short period planets such as these, we expect that in the absence of additional bodies, tidal forces should have already circularized the orbits

(e.g., Adams & Laughlin 2006). We also note that the other orbital parameters are changed by less than $1\text{-}\sigma$ when fixing $e = 0$, so in the absence of additional data, the assumption of circularized orbits is acceptable. We report the solutions with $e = 0$ in Table 3 and plot the best fit circular orbits in Figure 2.

4.3. Line Bisectors and Stellar Activity Indices

If the observed velocity variations were caused by a background blend (Mandushev et al. 2005) or star spots (Queloz et al. 2001), we would expect the shape of a star's line bisector to vary in phase with the radial velocities. A standard prescription for characterizing the shape of a line bisector is to measure the difference in relative velocity of the top and bottom of a line bisector; this difference is referred to as a line bisector span (see, e.g., Torres et al. 2005). To test against background blends or star spots, we computed the line bisector spans for all observations of Pr0201 and Pr0211. As illustrated in Figure 2, the bisector span variations are small ($\sigma_{BS} < 20 \text{ m s}^{-1}$) and are not correlated with the observed RV variations. As an additional check against activity induced RV variations, for each spectrum of Pr0201 and Pr0211 we also compute the S index – an indicator of chromospheric activity in the CaII H&K lines. We follow the procedure of Vaughan et al. (1978), but we note that our S indices are not calibrated to their scale; these are relative measurements. As shown in Figure 2, there is no correlation with orbital phase. These line bisector and S index comparisons strongly support the conclusion that the observed RV variations are caused by planetary companions.

4.4. Stellar and Planetary Properties

We used the spectroscopic classification technique Stellar Parameter Classification (SPC; Buchhave et al. 2012) to determine effective temperature T_{eff} , surface gravity $\log g$, projected rotational velocity $v \sin i$, and metallicity $[\text{m}/\text{H}]$ for each of our target stars. In essence, SPC cross correlates an observed spectrum against a grid of synthetic spectra, and uses the correlation peak heights to fit a 3-dimensional surface in order to find the best combination of atmospheric parameters ($v \sin i$ is fit iteratively since it is only weakly correlated to changes in the other parameters). We used the CfA library of synthetic spectra, which are based on Kurucz model atmospheres (Kurucz 1992) calculated by John Laird for a linelist compiled by Jon Morse. Like other spectroscopic classification techniques, SPC can be limited by degeneracy between parameters, notably T_{eff} , $\log g$, and $[\text{m}/\text{H}]$, but in this case we can enforce the known cluster metallicity to partially break that degeneracy. Though we leave detailed description of the ensemble sample for a subsequent paper, from an analysis of the 53 stars in our sample, we calculated a cluster metallicity of $[\text{m}/\text{H}] = +0.187 \pm 0.038$. This value is consistent with previous estimates (e.g., $+0.27 \pm 0.10$, Pace et al. 2008).

Regarding the planet hosts Pr0201 and Pr0211 in particular, we note that our derived temperatures of 6174 K and 5326 K are in agreement with published spectral types (F7.5 and G9.3; Kraus & Hillenbrand 2007), and that their individual SPC-derived metallicities ($+0.18 \pm 0.08$ and $+0.19 \pm 0.08$) are consistent with the median

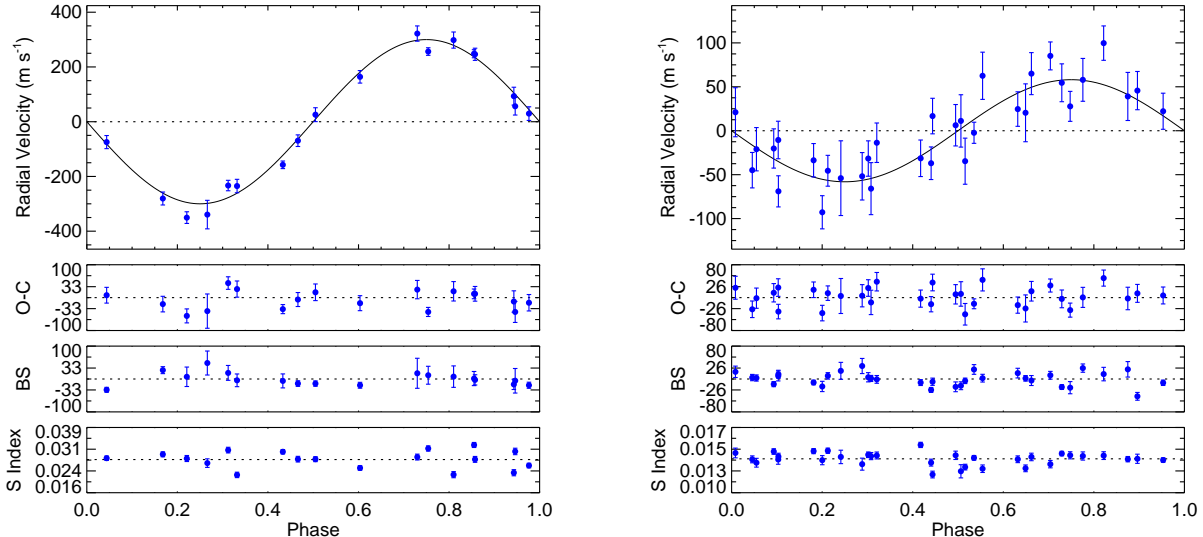


FIG. 2.— Orbital solutions for Pr0211 (left) and Pr0201 (right). The panels, from top to bottom, show the relative RVs, best-fit residuals, bisector span variations, and relative S index values. RV error bars represent the internal errors, and do not include astrophysical jitter, although 13 m s^{-1} jitter was assumed in the orbital fit. The solid curve shows the best-fit orbital solution. The orbital parameters are listed in Table 3.

of the cluster. Detailed heavy-element abundance analyses of Pr0201 are reported in Pace et al. (2008) and Maiorca et al. (2011).

We used the stellar parameters from SPC and the known age of Praesepe in conjunction with the Yonsei-Yale stellar models (Yi et al. 2001) to extract the stellar masses and radii. We found that the $\log g$ values indicated by the isochrone fits were slightly more than $1\text{-}\sigma$ lower than the SPC values, but it is possible that the formal errors for SPC are too small and/or that the stellar models are inaccurate for these somewhat young and active stars. We iterated the SPC analysis, this time fixing both the cluster metallicity and the $\log g$ from the isochrone fit. This resulted in a slightly lower T_{eff} , and the subsequent isochrone fit was consistent with all of the SPC parameters. Using an age of 578 Myr (Delorme et al. 2011), we adopted stellar masses and radii from the isochrone fits ($M_* = 1.234 \pm 0.034 M_\odot$, $R_* = 1.167 \pm 0.121 R_\odot$ for Pr0201; $M_* = 0.952 \pm 0.040 M_\odot$, $R_* = 0.868 \pm 0.078 R_\odot$ for Pr0211), but caution that the formal errors on stellar and planetary masses and radii do not encompass any potential systematics. The estimates of the stellar masses provide lower limits on the masses of the planets of $0.540 \pm 0.039 M_{\text{Jup}}$ for Pr0201b and $1.844 \pm 0.064 M_{\text{Jup}}$ for Pr0211b. Table 3 lists all of the stellar and planetary properties.

5. DISCUSSION

Our discovery of two hot Jupiters in Praesepe confirms that short-period planets do exist in open clusters. Moreover, assuming these gas giants formed beyond the snow-line, the planets have migrated to nearly circular short period orbits in 600 Myr. Although a more complete analysis that takes into account the detection limits of our entire sample is called for, we can already place some constraints on the hot Jupiter frequency in Praesepe. If we make the assumption that the observations of the other 51 stars in our sample can completely rule

TABLE 3
STELLAR AND PLANETARY PROPERTIES

	Pr0201	Pr0211
Orbital Parameters		
P [days]	4.4264 ± 0.0070	2.1451 ± 0.0012
T_c [BJD]	2455992.861 ± 0.053	2456013.9889 ± 0.0072
K [m s^{-1}]	58.1 ± 4.1	299.9 ± 6.1
e	0	0
γ [km s^{-1}]	34.035 ± 0.101	35.184 ± 0.198
Stellar and Planetary Properties		
M_* [M_\odot]	1.234 ± 0.034	0.952 ± 0.040
R_* [R_\odot]	1.167 ± 0.121	0.868 ± 0.078
$T_{\text{eff},*}$ [K] ^a	6174 ± 50	5326 ± 50
$\log g_*$ [dex] ^a	4.41 ± 0.10	4.55 ± 0.10
$v \sin i$ [km s^{-1}]	9.6 ± 0.5	4.8 ± 0.5
$[m/H]$ [dex] ^a	0.187 ± 0.038	0.187 ± 0.038
Age [Myr] ^b	578 ± 49	578 ± 49
$M_p \sin i$ [M_{Jup}]	0.540 ± 0.039	1.844 ± 0.064

NOTE. — The orbital parameters correspond to the best fit circular orbit (see Section 4.2).

^a From the final SPC iteration. $[m/H]$ was fixed to the mean cluster metallicity calculated from an SPC analysis of our 53 stars. See Section 4.4.

^b From Delorme et al. (2011).

out the presence of short-period, massive planets, then we obtain a lower limit on the hot Jupiter frequency in Praesepe: $(2^{+2.6}_{-1.3})/53$; at least $3.8^{+5.0}_{-2.4}\%$ of all single FGK cluster members host a hot Jupiter (Poisson errors were calculated following the prescription in Gehrels 1986). While this number is slightly higher than the frequency for field stars ($1.20 \pm 0.38\%$; Wright et al. 2012), it is consistent with that expected from the enriched metallicity environment of Praesepe.

Uncertainties in planetary properties are most often limited by determination of properties of their host stars, but planets in clusters – particularly those that transit their host stars – can yield greatly reduced observational uncertainties. The observable transit parameter a/R_* constrains the stellar $\log g$ (Sozzetti et al. 2007), and the

cluster's mean metallicity can be determined more precisely than that of any one star. Accurate $\log g$ and $[m/H]$ values will also improve the spectroscopic T_{eff} estimates by breaking the degeneracy between the three parameters. When combined with the cluster age and distance, the resulting range of allowed masses and radii from stellar models would be greatly reduced. The precision in the stellar properties would propagate to an extremely precise planetary mass, radius, and age, providing a better test for models of planetary structure and evolution. Just as they have played an important role in the calibration of stellar properties, open clusters

hold great promise as laboratories to explore properties of exoplanets at various ages and with great precision.

This material is based upon work supported by the National Aeronautics and Space Administration (NASA) under Grant No. NNX11AC32G issued through the Origins of Solar Systems program. D. W. L. acknowledges partial support from NASA's Kepler mission under Cooperative Agreement NNX11AB99A with the Smithsonian Astrophysical Observatory.

Facility: FLWO:1.5m (TRES)

REFERENCES

- Adams, F. C. & Laughlin, G. 2003, *Icarus*, 163, 290
 Adams, F. C. & Laughlin, G. 2006, *ApJ*, 649, 1004
 An D., Terndrup, D. M., & Pinsonneault, M. H. 2007, *ApJ*, 671, 1640
 Bouvier, J., Duchene, G., Mermilliod, J. C., & Simon, T. 2001, *A&A*, 375, 989
 Bressert E., Bastian, N., & Gutermuth, R. 2011, JENAM conference, arXiv:1102.0565
 Buchhave, L. A., et al. 2010, *ApJ*, 720, 1118
 Buchhave, L. A., et al. 2012, *Nature*, 486, 375
 Carpenter, J. M., Mamajek, E. E., Hillenbrand, L. A., & Meyer, M. R. 2006, *ApJ*, 651, 49
 Debes, J. H. & Jackson, B. 2010, *ApJ*, 723, 1703
 Delorme, P., et al. 2011, *MNRAS*, 413, 2218
 Eisner, J. A., Plambeck, R. L., Carpenter, J. M., Corder, S. A., Qi, C., & Wilner, D. 2008, *ApJ*, 683, 304
 Fischer, D. A. & Valenti, J. 2005, *ApJ*, 622, 1102
 Fűrész, G. 2008, Ph.D. thesis, University of Szeged, Hungary
 Gehrels, N. 1986, *ApJ*, 303, 336
 Gáspár, A., et al. 2009, *ApJ*, 697, 1578
 Goldreich, P. & Tremaine, S. 1980, *ApJ*, 241, 425
 Hambly, N. C., Steele, I. A., Hawkins, M. R. S., & Jameson, R. F. 1995, *MNRAS*, 273, 505
 Hartman, J. D., et al. 2009, *ApJ*, 695, 336
 Johnson, J. A., Aller, K. M., Howard, A. W., & Crepp, J. R. 2010, *PASP*, 122, 905
 Kraus, A. L. & Hillenbrand, L. A. 2007, *AJ*, 134, 2340
 Kurucz, R. L. 1992, *IAUS*, 149, 225
 Lin, D. N. C., Bodenheimer, P., & Richardson, D. C. 1996, *Nature*, 380, 606
 Lovis, C. & Mayor, M. 2007, *A&A*, 472, 657
 Lubow, S. H., & Ida, S. 2010, in *Exoplanets*, ed. S. Seager (Tucson, AZ: Univ. Arizona Press), 347
 Maiorca, E., et al. 2011, *ApJ*, 736, 120
 Mandushev, G., et al. 2005, *ApJ*, 621, 1061
 Mermilliod, J.-C., Mayor, M., & Udry, S. 2009, *A&A*, 498, 949
 Mochejska, B. J., et al. 2006, *AJ*, 131, 1090
 Pace, G., Pasquini, L., & Francois, P. 2008, *A&A*, 489, 403
 Pasquini, L., et al. 2012, *A&A*, in press (arXiv:1206.5820).
 Patience, J., Ghez, A. M., Reid, I. N., & Matthews, K. 2002, *AJ*, 123, 1570
 Paulson, D. B., Cochran, W. D., & Hatzes, A. P. 2004, *AJ*, 127, 3579
 Pepper, J., et al. 2008, *AJ*, 135, 907
 Queloz, D., et al. 2001, *A&A*, 379, 279
 Santos, N. C., Israelian, G., & Mayor, M. 2004, *Planetary Systems in the Universe*, 202, 118
 Sato, B., et al. 2007, *ApJ*, 661, 527
 Sozzetti, A., Torres, G., Charbonneau, D., Latham, D. W., et al. 2007, *ApJ*, 664, 1190
 Torres, G., Konacki, M., Sasselov, D. D., & Jha, S. 2005, *ApJ*, 619, 558
 van Saders, J. L. & Gaudi, B. S. 2011, *ApJ*, 729, 63
 Vaughan, A. H., Preston, G. W., & Wilson, O. C. 1978, *PASP*, 90, 267
 Wright, J. T., et al. 2011, *PASP*, 123, 412
 Wright, J. T., et al. 2012, *ApJ*, in press (arXiv:1205.2273).
 Yi, S., et al. 2001, *ApJS*, 136, 417
 Zakamska, N. L., Pan, M., & Ford, E. B. 2011, *MNRAS*, 410, 1895